IEEE Access
Multidisciplinary | Rapid Review | Open Access Journal

Received February 22, 2021, accepted March 8, 2021, date of publication March 17, 2021, date of current version March 23, 2021.

Digital Object Identifier 10.1109/ACCESS.2021.3066629

Resolvable Cluster Target Tracking Based on the DBSCAN Clustering Algorithm and Labeled RFS

XIRUI XUE, SHUCAI HUANG, JIAHAO XIE, JIASHUN MA, AND NING LI
Air and Missile Defense College, Air Force Engineering University, Xi'an 710051, China
Corresponding author: Xirui Xue (rayngu@126.com)

This work was supported in part by the Young Talent Support Project for Military Science and Technology under Grant 18-JC-JQ-QT-007.

ABSTRACT When a sensor can resolve the members in a cluster, it is difficult to accurately track each target due to cooperative interaction among the targets. In this paper, we research the tracking problem of resolvable cluster targets with cooperative interaction. Firstly, we use the stochastic differential equation to model the cluster coordination rules, and the state equation of the single target in the cluster is derived. On this basis, a Bayes recursive filter tracking method based on the combination of the DBSCAN clustering algorithm and the δ-GLMB filter is proposed. In the δ-GLMB filter prediction stage, the DBSCAN algorithm is used to determine the cluster where the target is located in real time. Then, the collaborative noise of the target is estimated, which will be used as the input to correct the prediction state of the target. The simulation and experiment results demonstrate the effectiveness of the proposed algorithm when the cluster is splitting, merging, and in reorganization.

INDEX TERMS Resolvable cluster target tracking, cooperative interaction modeling, stochastic differential equation, DBSCAN clustering algorithm, δ-GLMB filter.

I. INTRODUCTION

With the continuous improvement of cluster control technology as well as unmanned autonomous technology, there is a pressing need for accurate, timely, and efficient ways of tracking cluster targets. In the process of movement, there are cooperative interactions within a cluster, and there are also behaviors among clusters, such as splitting and merging. When the sensor is far from the cluster and the targets in the cluster cannot be resolved, the cluster extension is usually modeled as a random matrix that obeys the inverse Wishart distribution [1]. The cluster is usually tracked as a whole. When the targets in the cluster become fully resolvable for the sensor, the sensor can accurately track the targets based on an accurate estimation of the cooperative interactions among them. Reference [2] uses a Markov chain Monte Carlo (MCMC) method to track the coordinated groups. This method is able to detect and track targets within groups as well as to infer the correct group structure over time. Reference [3]–[5] use an adjacency matrix to establish the coordination rule within clusters, and the interaction is modeled as collaborative noise. In these References, the multi-target Bayes recursive filter is used to track a cluster with a fixed structure, and good results are obtained. At present, the difficulties of cluster target tracking focus mainly three aspects: target kinematic modeling in the cluster, cluster state estimation, and multi-target tracking in the clutter environment.

In terms of target kinematic modeling in the cluster, Reynolds summarizes the three coordination rules of separation, alignment, and cohesion among cluster members through research of the movement of organisms with cluster behaviors [6]. Viscek proposes the Viscek model [7], which illustrates that the velocity of the target in the cluster can be consistent when each target adjusts its velocity direction to the average value of the velocity direction of the targets in its neighborhood. Couzin, *et al.* study the phenomenon of effective guidance and group decision-making and discuss the splitting phenomenon of clusters [8]. In addition, the interaction model based on the force between members is also a cluster motion modeling method. It is a dynamic modeling method based on Newton's second law. The model abstracts the cooperative interaction between members in a cluster as "force", which can be decomposed into two parts: position coordination force and speed coordination force. The individual completes its maneuver under the resultant force of surrounding members [9]. Usually, force is generated from the potential field [10], [11] along the direction of the negative

The associate editor coordinating the review of this manuscript and approving it for publication was Prakasam Periasamy.

gradient of the potential function and follows the principles of long-ranged attraction and short-ranged repulsion.

The cluster state estimation problem can be divided into two parts: target clustering and cluster structure estimation. As is evident, the correct clustering of targets in the field of view is the basis for estimating interactions. There are many ways to cluster targets. They include data-based clustering algorithms and parameter-likelihood-based clustering algorithms [12]. Data-based clustering algorithms include hierarchical clustering [13] and partitional clustering (e.g., the K-means estimator [14]). Density-based spatial clustering of applications with noise (DBSCAN) is a typical data-based clustering algorithm [15], [16], which can be used to solve clustering problems with uncertain data. The dynamic estimation of a cluster structure is an important part of cluster state estimation. Its methods mainly include two types. One is based on transition probability, and the other is based on evolution models [17]. Reference [18], [19] establishes a similarity evaluation function between different cluster structures to calculate the transition probability of cluster structures. In Reference [20], Gning uses evolving networks to model the dynamic evolution of a cluster structure and estimates it by the Monte Carlo method.

After obtaining the targets' clustering and cluster structure, we can calculate the cooperative interaction through the interaction relationship between the targets. The next problem to be solved is the multi-target tracking problem in the clutter environment. When there is a large amount of clutter in the sensor field of view, the hypothesis correlation filtering algorithm represented by joint probabilistic data correlation (JPDA) [21], [22] is difficult to achieve accurate multi-target tracking. However, the multi-target Bayes recursive filter constructed by Mahler can effectively solve the tracking problem in this case. These methods include the probability hypothesis density (PHD) filter [23], [24], the cardinalized PHD filter (CPHD) [25], [26], the multi-target multi-Bernoulli (MeMBer) filter [27], [28], and the generalized label multi-Bernoulli (GLMB) filter [29], [30], and others.

In this paper, based on the combination of basic rules of cluster motion and the CV model, we derive a state space motion model for single target in the cluster, which can be directly applied to the multi-target Bayes recursive filter. According to the characteristics of the cluster target, we define a new distance as the distance measure of the DBSCAN algorithm. By setting changeable parameter, we combine the DBSCAN clustering algorithm with the δ-GLMB filter to achieve target tracking and cluster state estimation at the same time.

The content of this paper is arranged as follows: Section 2 derives the motion state equation of each independent target in the cluster; Section 3 introduces the DBSCAN clustering algorithm and combines it with the GLMB filtering process; three simulations we carried out to verify the effectiveness of the proposed method are described in Section 4; and Section 5 summarizes the paper.

II. CLUSTER MOTION MODEL

A. STOCHASTIC DIFFERENTIAL EQUATION MODEL

The members in the cluster are guided by simple rules and produce collaborative movement by cooperative interaction mechanisms. The members in the cluster respond to the behaviors of other members in the cluster, which ultimately results in a global alignment of their velocity vectors, convergence of their speeds to a common speed, no collisions within the cluster, and the minimization of the potential function of the cluster [31].

The acceleration of each target should be calculated based on the positions and velocities of the surrounding targets in the cluster due to their cooperative interactions. A stochastic differential equation (SDE) [32] can effectively describe the coordination rules, which will be placed in discrete time without approximate error. Equation (1) is the SDE model of the ith target in the cluster. In the Equation, separation and cohesion are modeled as the potential force, and the alignment is modeled as a restoring force which adjusts the target velocity closer to the average velocity $f(\dot{\boldsymbol{s}}_t)$.

$$d\dot{\boldsymbol{s}}_{t,i} = \left\{-\alpha\left[\dot{\boldsymbol{s}}_{t,i} - f(\dot{\boldsymbol{s}}_t)\right] + \beta r_i(\boldsymbol{s}_{t,i})\right\} dt + d\boldsymbol{W}^s_{t,i} + d\boldsymbol{B}^s_t \tag{1}$$

Here, $\boldsymbol{s}_{t,i} \in \boldsymbol{R}^d$ is the position of the ith target in a cluster at time t, and $\dot{\boldsymbol{s}}_{t,i}$ is its velocity. α is the velocity control parameter that reflects the strength of the alignment effect on acceleration. Similarly to α, β is the potential force control parameter that reflects the strength of the separation and cohesion effect on acceleration. $\boldsymbol{W}^s_{t,i}$ is a d-dimensioned random vector, which models ith target motion random noise. $\boldsymbol{B}^s_t$ is another d-dimensioned random vector, modeling overall randomness in the motion of the cluster as a whole. $f(\dot{\boldsymbol{s}}_t)$ indicates the average velocity of all targets in the cluster. Assuming the number of cluster members is N, we arrive at the following formula:

$$f(\dot{\boldsymbol{s}}_t) = \frac{1}{N}\sum_{j=1}^{N}\dot{\boldsymbol{s}}_{t,j} \tag{2}$$

The introduction of $f(\dot{\boldsymbol{s}}_t)$ realizes the alignment of the members within the cluster and ensures their information transmission. From the perspective of graph theory, this makes the cluster topology have weak connectivity, which is critical for the velocity of cluster members to achieve consistency. $r_i(\boldsymbol{s}_{t,i})$ is the resultant force of the potential force received by the i th target. The expression is as follows:

$$r_i(\boldsymbol{s}_t) = \sum_{\forall j, j\neq i} r(\boldsymbol{s}_{t,i}, \boldsymbol{s}_{t,j}) \tag{3}$$

Here, $r(\boldsymbol{s}_{t,i}, \boldsymbol{s}_{t,j})$ indicates the potential force generated by the jth target on the ith target, and its magnitude is determined by the potential function $U_j(\cdot)$ and the Euclidean distance between the two targets.

If the cluster topology has weak connectivity and the randomness in motion does not significantly affect the cooperative interaction between members, the cluster members

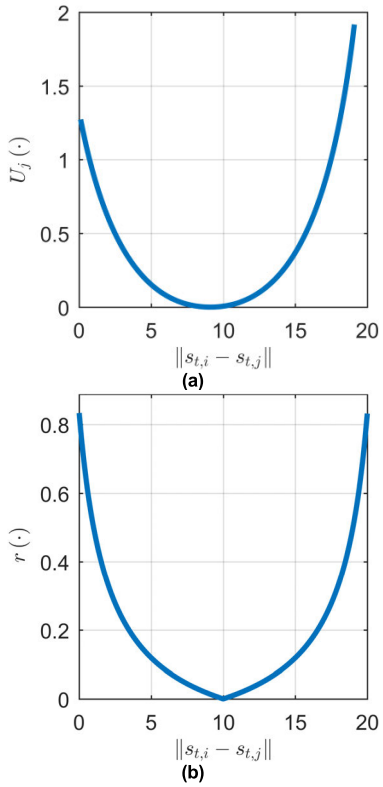

FIGURE 1. The variation of $U_j(\cdot)$ and $r(\cdot)$ with distance between two targets ($R_{11} = R_{12} = R_{21} = R_{22} = 2$, $d_r = 10$, $d_m = 20$). (a) is the variation of $U_j(\cdot)$; (b) is the variation of $r(\cdot)$.

will gradually obtain a consistent velocity to form a collective motion on the condition that $U_j(\cdot)$ is a consequent differentiable non-negative function and the only minimum value can be obtained at a certain point. See Appendix for the proof.

$U_j(\cdot)$ can be defined as Equation (4), as shown at the bottom of the next page. It is easy to prove that $\left.\frac{dU_j(z)}{dz}\right|_{z=d_r^-} = \left.\frac{dU_j(z)}{dz}\right|_{z=d_r^+} = 0$, and it has a minimum at $\|s_{t,i} - s_{t,j}\| = d_r$. where d_r is the balance distance between two targets and d_m is the maximum distance that targets can generate potential force. When the distance between the two targets is less than d_r, the potential force is repulsive force. Otherwise, the potential force is attractive force. R_{11}, R_{12}, R_{21}, and R_{22} are the control parameters of the potential field intensity. Setting $R_{11} = R_{12} = R_{21} = R_{22} = 2$, $d_r = 10$, and $d_m = 20$, the potential function is shown in Figure 1(a).

The potential force received by ith target can be defined as the negative gradient of the potential function. Based on Equation (4), the expression of $r\left(s_{t,i}, s_{t,j}\right)$ is shown as Equation (5), as shown at the bottom of the next page. Setting the parameters as above, Figure 1(b) shows the variation of potential force with the separation distance between two targets.

R_{12} and R_{22} should be set to non-zero parameters. Then, the magnitude of repulsive force will be limited to $\frac{R_{11}d_r}{R_{12}(d_r+R_{12})}$ when two targets are very close together. The magnitude of attractive force will be limited to $\frac{R_{21}(d_m-d_r)}{R_{22}(d_m-d_r+R_{22})}$ when the distance between the two targets approaches d_m. This can avoid sudden excessive changes in the target position and velocity due to the potential force. This restriction is reasonable and necessary for realistic cluster targets. Nevertheless, the restriction must be set reasonably. In some cases, if it is set too small, cluster members may collide with each other.

A linear SDE for the joint target state can be written as

$$d\boldsymbol{X}_t = \boldsymbol{A}\boldsymbol{X}_t dt + \boldsymbol{R}dt + \boldsymbol{B}d\boldsymbol{W}_t + \boldsymbol{C}d\boldsymbol{B}_t \tag{6}$$

Here, $\boldsymbol{X}_t = \left[x_{t,1}, \dot{x}_{t,1}, y_{t,1}, \dot{y}_{t,1}, \cdots, x_{t,N}, \dot{x}_{t,N}, y_{t,N}, \dot{y}_{t,N}\right]^T$. Matrix $\boldsymbol{A} \in \boldsymbol{R}^{4N\times 4N}$ is defined as follows:

$$\boldsymbol{A} = \begin{bmatrix} A_1 & A_2 & \cdots & A_2 \\ A_2 & A_1 & \cdots & A_2 \\ \vdots & & \ddots & \vdots \\ A_2 & A_2 & \cdots & A_1 \end{bmatrix}$$

$$\boldsymbol{A}_1 = \begin{bmatrix} 0 & 1 & 0 & 0 \\ 0 & \frac{(1-N)\alpha}{N} & 0 & 0 \\ 0 & 0 & 0 & 1 \\ 0 & 0 & 0 & \frac{(1-N)\alpha}{N} \end{bmatrix}$$

$$\boldsymbol{A}_2 = \begin{bmatrix} 0 & 0 & 0 & 0 \\ 0 & \frac{\alpha}{N} & 0 & 0 \\ 0 & 0 & 0 & 0 \\ 0 & 0 & 0 & \frac{\alpha}{N} \end{bmatrix} \tag{7}$$

Matrix $\boldsymbol{R} \in \boldsymbol{R}^{4N\times 1}$ is defined as follows:

$$\boldsymbol{R} = \left[0, \beta r_{i,x}(s_t), 0, \beta r_{i,y}(s_t), \cdots, 0, \beta r_{N,x}(s_t), 0, \beta r_{N,y}(s_t)\right]^T \tag{8}$$

Matrix $\boldsymbol{B} \in \boldsymbol{R}^{4N\times 2N}$ is defined as follows:

$$\boldsymbol{B} = \begin{bmatrix} B_1 & 0 & \cdots & 0 \\ 0 & B_1 & \cdots & 0 \\ \vdots & & \ddots & \vdots \\ 0 & 0 & \cdots & B_1 \end{bmatrix} \boldsymbol{B}_1 = \begin{bmatrix} 0 & 0 \\ 1 & 0 \\ 0 & 0 \\ 0 & 1 \end{bmatrix} \tag{9}$$

Matrix $\boldsymbol{C} \in \boldsymbol{R}^{4N\times 2}$ is defined as follows:

$$\boldsymbol{C} = \left[B_1^T, B_1^T, \ldots, B_1^T\right]^T \tag{10}$$

The multidimensional motion random noises $\boldsymbol{W}_t$ and $\boldsymbol{B}_t$ are given as follows:

$$\boldsymbol{W}_t = \left[W_{t,1}^x, W_{t,1}^y, \cdots, W_{t,N}^x, W_{t,N}^y\right]^T \tag{11}$$

$$\boldsymbol{B}_t = \left[B_t^x, B_t^y\right]^T \tag{12}$$

We model the noise as random numbers that obey Gaussian distribution. The corresponding covariance matrices are $\boldsymbol{Q}_W = diag\left[\sigma_x^2, \sigma_y^2, \cdots, \sigma_x^2, \sigma_y^2\right]$ and $\boldsymbol{Q}_B = diag\left[\sigma_g^2, \sigma_g^2\right]$. Since the two noises have the same form, we define a joint noise $\boldsymbol{M}_t$ with the covariance matrix $\boldsymbol{Q}_M = diag\left[\sigma_x^2, \sigma_y^2, \cdots, \sigma_x^2, \sigma_y^2, \sigma_g^2, \sigma_g^2\right]$. The matrix $\boldsymbol{D} \in R^{4N\times 2(N+1)}$ is defined as $\boldsymbol{D} = [\boldsymbol{B}, \boldsymbol{C}]$.

Equation (6) can be equivalently written as

$$d\boldsymbol{X}_t = \boldsymbol{A}\boldsymbol{X}_t dt + \boldsymbol{R}dt + \boldsymbol{D}d\boldsymbol{M}_t \tag{13}$$

According to Reference [32], the above SDE has an exact solution $\boldsymbol{X}_{t+\tau}$ at time $t+\tau$.

$$\boldsymbol{X}_{t+\tau} = e^{\boldsymbol{A}\tau}\boldsymbol{X}_t + \boldsymbol{R}\int_{s=t}^{s=t+\tau} e^{\boldsymbol{A}(t+\tau-s)}ds + \int_{s=t}^{s=t+\tau} e^{\boldsymbol{A}(t+\tau-s)}\boldsymbol{D}\boldsymbol{Q}_M\boldsymbol{D}^T(e^{\boldsymbol{A}(t+\tau-s)})^T ds \tag{14}$$

We define that the joint transition matrix is given by

$$\boldsymbol{F}_{ct}(\tau) = e^{\boldsymbol{A}\tau} \tag{15}$$

The joint covariance matrix of noise is given by

$$\boldsymbol{Q}_{ct}(\tau) = \int_{s=t}^{s=t+\tau} e^{\boldsymbol{A}(t+\tau-s)}\boldsymbol{D}\boldsymbol{Q}_M\boldsymbol{D}^T(e^{\boldsymbol{A}(t+\tau-s)})^T ds \tag{16}$$

The coefficient matrix of potential force is shown as

$$\boldsymbol{E}_{ct}(\tau) = \int_{s=t}^{s=t+\tau} e^{\boldsymbol{A}(t+\tau-s)}ds \tag{17}$$

Let $z = s - t$, then $\boldsymbol{E}_{ct}(\tau) = \int_{s=t}^{s=t+\tau} e^{\boldsymbol{A}(t+\tau-s)}ds = \int_{z=0}^{z=\tau} e^{\boldsymbol{A}(\tau-z)}dz$. We can find that $\boldsymbol{E}_{ct}(\tau)$ has nothing to do with the initial moment of the target state transition, but only with τ. Similarly to $\boldsymbol{E}_{ct}(\tau)$, $\boldsymbol{Q}_{ct}(\tau)$ also has this property.

When the sampling time interval $\tau = 1$, in order to simplify the notation, we write the matrices $\boldsymbol{F}_{ct}(1)$, $\boldsymbol{E}_{ct}(1)$, and $\boldsymbol{Q}_{ct}(1)$ as $\boldsymbol{F}_{ct}$, $\boldsymbol{E}_{ct}$, and $\boldsymbol{Q}_{ct}$, respectively. Based on the above results, the discrete-time state equation of the joint target is written as follows:

$$\boldsymbol{X}_{k+1} = \boldsymbol{F}_{ct}\boldsymbol{X}_k + \boldsymbol{E}_{ct}\boldsymbol{R} + \boldsymbol{\Gamma}_{ct}\boldsymbol{w}_k \tag{18}$$

Here, $\boldsymbol{\Gamma}_{ct}$ is the state noise factor matrix, $\boldsymbol{w}_k$ is Gaussian noise with the covariance matrix $\boldsymbol{Q}_{ct}$.

B. STATE SPACE MODEL

In order to track a single target, we need to obtain the state equation of the single target by separating the target joint state equation and transforming it into a general form that is more suitable for tracking algorithms.

The solution of $\boldsymbol{F}_{ct}$ is shown as follows. We can find that $\boldsymbol{F}_{ct}$ is composed of $\boldsymbol{F}_{ct}^s$ and $\boldsymbol{F}_{ct}^c$, which are given by

$$\begin{aligned}
\boldsymbol{F}_{ct} &= \begin{bmatrix} \boldsymbol{F}_{ct}^s & \boldsymbol{F}_{ct}^c & \cdots & \boldsymbol{F}_{ct}^c \\ \boldsymbol{F}_{ct}^c & \boldsymbol{F}_{ct}^s & \cdots & \boldsymbol{F}_{ct}^c \\ \vdots & & \ddots & \vdots \\ \boldsymbol{F}_{ct}^c & \boldsymbol{F}_{ct}^c & \cdots & \boldsymbol{F}_{ct}^s \end{bmatrix} \\
\boldsymbol{F}_{ct}^s &= \begin{bmatrix} 1 & \boldsymbol{F}_{ct}(1,2) & 0 & 0 \\ 0 & \boldsymbol{F}_{ct}(2,2) & 0 & 0 \\ 0 & 0 & 1 & \boldsymbol{F}_{ct}(1,2) \\ 0 & 0 & 0 & \boldsymbol{F}_{ct}(2,2) \end{bmatrix} \\
\boldsymbol{F}_{ct}^c &= \begin{bmatrix} 0 & \dfrac{1-\boldsymbol{F}_{ct}(1,2)}{N-1} & 0 & 0 \\ 0 & \dfrac{1-\boldsymbol{F}_{ct}(2,2)}{N-1} & 0 & 0 \\ 0 & 0 & 0 & \dfrac{1-\boldsymbol{F}_{ct}(1,2)}{N-1} \\ 0 & 0 & 0 & \dfrac{1-\boldsymbol{F}_{ct}(2,2)}{N-1} \end{bmatrix}
\end{aligned} \tag{19}$$

The solution of $\boldsymbol{E}_{ct}$ has the same form as $\boldsymbol{F}_{ct}$. However, since the value of α is generally small, it can be considered that the influence of the potential force on the ith target is independent of other targets. Therefore, E_{ct}^s can be simplified to a constant matrix, and $\boldsymbol{E}_{ct}^c = \boldsymbol{O}_{4\times4}$.

$$\begin{aligned}
\boldsymbol{E}_{ct} &= \begin{bmatrix} \boldsymbol{E}_{ct}^s & \boldsymbol{E}_{ct}^c & \cdots & \boldsymbol{E}_{ct}^c \\ \boldsymbol{E}_{ct}^c & \boldsymbol{E}_{ct}^s & \cdots & \boldsymbol{E}_{ct}^c \\ \vdots & & \ddots & \vdots \\ \boldsymbol{E}_{ct}^c & \boldsymbol{E}_{ct}^c & \cdots & \boldsymbol{E}_{ct}^s \end{bmatrix} \\
\boldsymbol{E}_{ct}^s &= \begin{bmatrix} 1 & \dfrac{1}{2} & 0 & 0 \\ 0 & 1 & 0 & 0 \\ 0 & 0 & 1 & \dfrac{1}{2} \\ 0 & 0 & 0 & 1 \end{bmatrix}
\end{aligned} \tag{20}$$

The solution of $\boldsymbol{Q}_{ct}$ also has the same form as $\boldsymbol{F}_{ct}$. Under the premise that the randomness in motion does not significantly affect the cooperative interaction, the noise covariance matrix of the ith target is $\boldsymbol{Q}_{ct}^s$.

$$U_j\left(\left\|\boldsymbol{s}_{t,i}-\boldsymbol{s}_{t,j}\right\|\right) = \begin{cases} R_{11}\ln\dfrac{d_r+R_{12}}{\left\|\boldsymbol{s}_{t,i}-\boldsymbol{s}_{t,j}\right\|+R_{12}} + \dfrac{R_{11}}{d_r+R_{12}}\left(\left\|\boldsymbol{s}_{t,i}-\boldsymbol{s}_{t,j}\right\|-d_r\right) & \left\|\boldsymbol{s}_{t,i}-\boldsymbol{s}_{t,j}\right\| \le d_r \\ R_{21}\ln\dfrac{d_m-d_r+R_{22}}{-\left\|\boldsymbol{s}_{t,i}-\boldsymbol{s}_{t,j}\right\|+d_m+R_{22}} + \dfrac{R_{21}}{d_m-d_r+R_{22}}\left(d_r-\left\|\boldsymbol{s}_{t,i}-\boldsymbol{s}_{t,j}\right\|\right) & d_r < \left\|\boldsymbol{s}_{t,i}-\boldsymbol{s}_{t,j}\right\| < d_m \end{cases} \tag{4}$$

$$r\left(\boldsymbol{s}_{t,i},\boldsymbol{s}_{t,j}\right) = -grad\left(U_j\left(\left\|\boldsymbol{s}_{t,i}-\boldsymbol{s}_{t,j}\right\|\right)\right) = \begin{cases} \dfrac{R_{11}}{\left\|\boldsymbol{s}_{t,i}-\boldsymbol{s}_{t,j}\right\|+R_{12}} - \dfrac{R_{11}}{d_r+R_{12}} & \left\|\boldsymbol{s}_{t,i}-\boldsymbol{s}_{t,j}\right\| \le d_r \\ \dfrac{-R_{21}}{d_m-\left\|\boldsymbol{s}_{t,i}-\boldsymbol{s}_{t,j}\right\|+R_{22}} + \dfrac{R_{21}}{d_m-d_r+R_{22}} & d_r < \left\|\boldsymbol{s}_{t,i}-\boldsymbol{s}_{t,j}\right\| < d_m \end{cases} \tag{5}$$

From the above solution, a single target state equation can be given by

$$\boldsymbol{x}_{k+1,i} = \boldsymbol{F}^{s}_{ct}\boldsymbol{x}_{k,i} + \boldsymbol{F}^{c}_{ct}\sum_{\forall j, j\neq i}\boldsymbol{x}_{k,j} + \boldsymbol{c}_{k,i} + \boldsymbol{\Gamma}_k\boldsymbol{w}_{k,i} \quad (21)$$

Here, (22) and (23), as shown at the bottom of the next page $\boldsymbol{w}_{k,i}$ is Gaussian noise with covariance matrix $\boldsymbol{Q}^{s}_{ct}$.

In Reference [4], a new collaborative noise is proposed:

$$\boldsymbol{w}^{0}_{k,i} = \Delta\boldsymbol{c}_{k,i} + \boldsymbol{\Gamma}_k\boldsymbol{w}_{k,i} \quad (24)$$

where

$$\Delta\boldsymbol{c}_{k,i} = \sum_{\forall j, j\neq i}\boldsymbol{\omega}_k\left[\frac{\boldsymbol{c}_{k,(i,j)}}{\boldsymbol{\omega}_k} - \boldsymbol{F}_k\left(\dot{\boldsymbol{x}}_{k,i} - \dot{\boldsymbol{x}}_{k,j}\right)\right] \quad (25)$$

$$\dot{\boldsymbol{x}}_{k,i} = \left[0, \dot{x}_{k,i}, 0, \dot{y}_{k,i}\right]^T \quad (26)$$

$$\boldsymbol{\omega}_k = \frac{1}{N-1}\left(\boldsymbol{I}_{4\times 4} - diag\left[\boldsymbol{F}_{ct}(1,2), \boldsymbol{F}_{ct}(2,2), \boldsymbol{F}_{ct}(1,2), \boldsymbol{F}_{ct}(2,2)\right]\right) \quad (27)$$

Equation (24) suggests that the new noise is composed of the target's own motion noise and cooperative interaction. Based on the framework of the CV model, the single target tracking equation in the cluster is proposed as follows:

$$\boldsymbol{x}_{k+1,i} = \boldsymbol{F}_k\boldsymbol{x}_{k,i} + \boldsymbol{w}^{0}_{k,i} \quad (28)$$

$$\boldsymbol{z}_{k+1,i} = \boldsymbol{H}_k\boldsymbol{x}_{k+1,i} + \boldsymbol{v}_{k+1,i} \quad (29)$$

In Equation (28),

$$\boldsymbol{F}_k = \begin{bmatrix} 1 & 1 & 0 & 0 \\ 0 & 1 & 0 & 0 \\ 0 & 0 & 1 & 1 \\ 0 & 0 & 0 & 1 \end{bmatrix}.$$

Assuming that the cooperative interaction is random and satisfies the Gaussian distribution as Equation (30), collaborative noise $\boldsymbol{w}^{0}_{k,i}$ is Gaussian with $\boldsymbol{\mu}^{0}_{k,i}$ and covariance $\boldsymbol{Q}^{0}_{k,i}$.

$$\boldsymbol{c}_{k,(i,j)} \sim N\left(\bar{\boldsymbol{c}}_{k,(i,j)}, \boldsymbol{S}_{k,(i,j)}\right) \quad (30)$$

$$\boldsymbol{w}^{0}_{k,i} \sim N\left(\boldsymbol{\mu}^{0}_{k,i}, \boldsymbol{Q}^{0}_{k,i}\right) \quad (31)$$

$$\boldsymbol{\mu}^{0}_{k,i} = \sum_{\forall j, j\neq i}\boldsymbol{\omega}_k\left[\frac{\bar{\boldsymbol{c}}_{k,(i,j)}}{\boldsymbol{\omega}_k} - \boldsymbol{F}_k\left(\hat{\dot{\boldsymbol{x}}}_{k,i} - \hat{\dot{\boldsymbol{x}}}_{k,j}\right)\right] \quad (32)$$

$$\boldsymbol{Q}^{0}_{k,i} = \sum_{\forall j, j\neq i}\boldsymbol{S}_{k,(i,j)} + \boldsymbol{\omega}_k\boldsymbol{F}_k\left[\sum_{\forall j, j\neq i}\left(\boldsymbol{B}_{k,j} - \boldsymbol{B}_{k,i}\right)\right] \times\boldsymbol{F}^T_k\boldsymbol{\omega}^T_k + \boldsymbol{\Gamma}_k\boldsymbol{Q}^{s}_{ct}\boldsymbol{\Gamma}^T_k \quad (33)$$

Here, $\boldsymbol{B}_{k,i}$ is the covariance matrix of $\dot{\boldsymbol{x}}_{k,i}$.

The figure above illustrates the main process of transforming the joint state space model derived from SDE model to the single target state space model in CV framework. Firstly, we decompose the parameter matrix of joint state space model into state transition parameter matrix (superscript s) and cooperative parameter matrix (superscript c) of single target, and extract the cooperative force of single target as $\boldsymbol{c}_{k,i}$ to obtain single target state space model. Furthermore, in the framework of CV motion model, we transform the state space model of a single target, so that the state transition matrix of a single target is $\boldsymbol{F}_k$, and other cooperative effects and motion noise are combined into the defined cooperative noise $\boldsymbol{w}^{0}_{k,i}$. The derivation of single target state space model will be the basis of applying Bayesian filter to single target state estimation.

In measurement Equation (29),

$$\boldsymbol{H}_k = \begin{bmatrix} 1 & 0 & 0 & 0 \\ 0 & 0 & 1 & 0 \end{bmatrix}.$$

Measurement noise $\boldsymbol{v}_{k,i}$ is Gaussian white noise with covariance matrix $\boldsymbol{R}_k$.

Based on the above model, we set the parameters as shown in Table 1 and the collaborative motion of the cluster is shown in Figure 3(a). The velocity convergence of the targets is shown in Figure 3(b).

In the tracking process, we assume that the potential force equation between targets is a priori. We will apply it in the target state prediction stage. If the potential force equation is unknown, it must be estimated according to the filtering result of the target state. Usually, the potential force equation is based on the target state and motion information. A detailed discussion can be found in Reference [4].

TABLE 1. Simulation parameters for cluster motion.

Simulation Parameter	Symbol	Value
Actual number of targets	N	4
Number of simulation time steps	T	200
Cluster velocity control parameter	α	0.1
Potential field force control parameter	β	0.1
Balance distance	d_r	15
Maximum distance	d_m	30
Individual motion noise	σ_x	0.002
Cluster motion noise	σ_g	0.002
Control parameters of the potential field intensity	$\begin{bmatrix} R_{11} & R_{12} \\ R_{21} & R_{22} \end{bmatrix}$	$\begin{bmatrix} 4 & 3 \\ 4 & 1 \end{bmatrix}$

III. TARGET TRACKING METHOD

We divide the cluster target tracking into two problems: target state estimation and cluster state estimation. The target state estimation includes target motion states, the number of targets, and the cooperative relationship between the targets. The cluster state estimation mainly includes the division of clusters and the number of clusters in the field of view. It is obvious that an accurate estimation of the target state is the basis for an effective estimation of the cluster state. Meanwhile, correct cluster state estimation is the key to judging whether there is a cooperative interaction between two targets. In this section, a DBSCAN clustering algorithm based on the distance of target motion similarity is proposed. We apply this algorithm to the prediction step of the δ-GLMB filtering algorithm to achieve target and cluster state estimation at the same time.

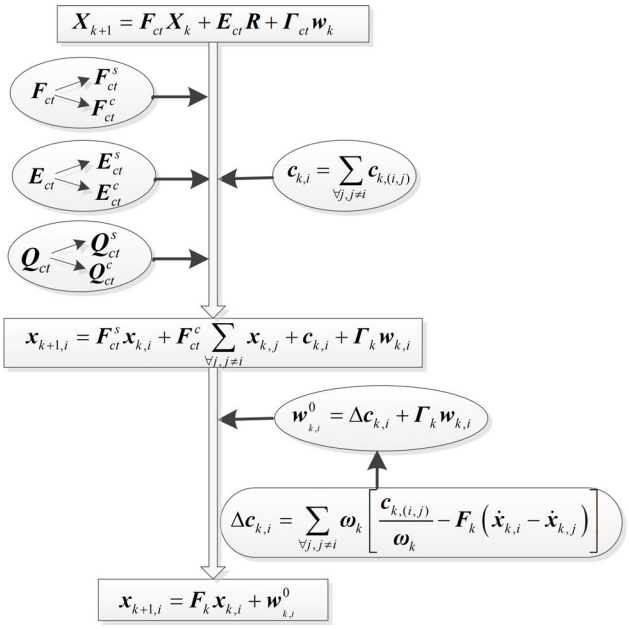

FIGURE 2. Transformation from SDE model to space state model.

A. DBSCAN CLUSTERING ALGORITHM

Probability based Bayesian filtering method is faced with the problem of distinguishing clutter from real measurement, so clustering algorithm must be more robust to filtering results. Because the coordination interaction between two targets within the same cluster changes in a U-shape, the targets that are far away from each other will be more attractive. If the wrong filtering value appears and it is far away from the real filtering value, the application of general clustering method may affect the estimation of the coordination interaction between targets. Density-based spatial clustering of application with noise (DBSCAN) is a common clustering algorithm for processing high-dimensional spatiotemporal data. It has the characteristics of high processing efficiency, effectively distinguishing noise points, and finding clusters of arbitrary shapes. Thus, the DBSCAN algorithm can enhance the accuracy of coordination interaction estimation with the help of noise recognition.

The core idea of the DBSCAN algorithm is to cluster the high-density areas of target point data into clusters and require each target in the cluster to reach a certain threshold in the number of adjacent targets within a given radius. According to the similarity metric, the result of clustering divides the temporal and spatial data with similarity in the target points into the same cluster, so that the difference in data similarity in the same cluster is as small as possible, and the difference between clusters is as large as possible.

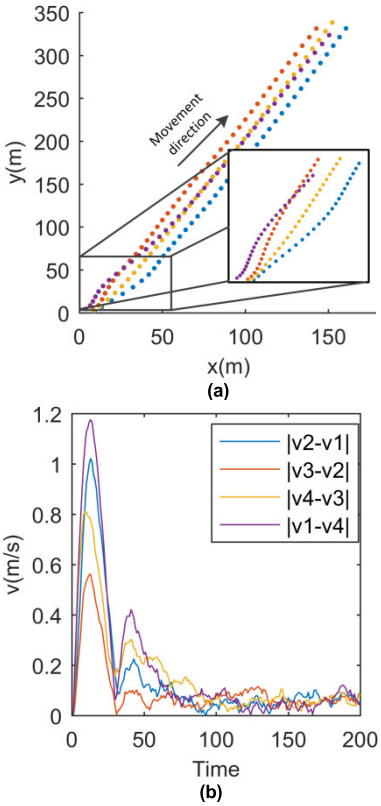

FIGURE 3. An example of cluster motion based on the above model. (a) is the trajectory of the cluster; (b) is the velocity convergence of the targets in the cluster.

The DBSCAN algorithm involves several important definitions: Eps-neighborhood, density, core point, border point, noise point, direct density-reachable, density-reachable, and density-connected. See Reference [15] for specific explanations.

Figure 4 is a clustering example of the DBSCAN algorithm. The radius of the circles is the cluster radius *Eps* and set $MinPts = 2$. In Figure 4, points 2, 3, 4, 5, and 6 have at least *MinPts* points in the neighborhood; thus they are core points. While point 1 has only 1 point in the neighborhood, it is a border point. There are no other points in the neighborhood of point 7. Therefore, point 7 is considered as a noise point. In summary, we can arrive at points $\{1, 2, 3, 4, 5, 6\}$ belonging to the same cluster.

We define a distance measure of target kinematic similarity $d(\cdot)$. $d(\cdot)$ uses a value between 0 and 1 to reflect the possibility that two targets belong to the same cluster. When $d(\cdot) = 1$, the two targets are considered to belong to two different clusters, and no cooperative interaction occurs. When $d(\cdot) = 0$, it is considered that the two targets have

$$c_{k,i} = \sum_{\forall j, j \neq i} c_{k,(i,j)} = \left[\beta r_{i,x}/2 \ \beta r_{i,x} \ \beta r_{i,y}/2 \ \beta r_{i,y} \right]^T \tag{22}$$

$$c_{k,(i,j)} = \left[\beta r_{i,x} \left(x_{k,i}, x_{k,j} \right)/2 \ \beta r_{i,x} \left(x_{k,i}, x_{k,j} \right) \ \beta r_{i,y} \left(x_{k,i}, x_{k,j} \right)/2 \ \beta r_{i,y} \left(x_{k,i}, x_{k,j} \right) \right]^T \tag{23}$$

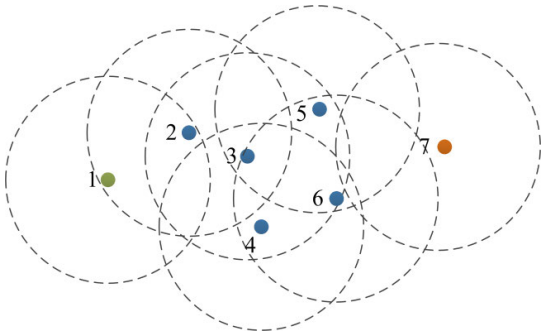

FIGURE 4. An illustration of the DBSCAN clustering algorithm.

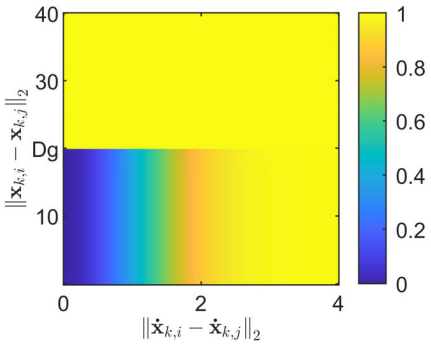

FIGURE 5. The variation of $d(\cdot)$ with R_v and R_d.

completely achieved cluster motion, and that they form part of the same cluster.

$$d\left(x_{k,i}, x_{k,j}\right) = 1 - (1 - sgn(R_d))\, e^{-\frac{R_v^2}{2\sigma_{R_v}^2}} \tag{34}$$

$$R_v = \sqrt{(\dot{x}_{k,i} - \dot{x}_{k,j})^2 + (\dot{y}_{k,i} - \dot{y}_{k,j})^2} \tag{35}$$

$$R_d = \max\left(0, \sqrt{(x_{k,i} - x_{k,j})^2 + (y_{k,i} - y_{k,j})^2} - D_g\right) \tag{36}$$

Here, R_v and R_d are the relative velocity and distance of a pair of targets, respectively. σ_{R_v} is the standard deviation of relative velocity; D_g describes the extent of the cluster.

Set $D_g = 20$, $\sigma_{R_v} = 1$. According to the above definition, the relationship between $d(\cdot)$ and the speed and location of two targets is shown in Figure 5. When the location distance between the two targets is less than D_g, the distance $d(\cdot)$ between two targets increases with the speed distance of two targets. And the possibility that two targets belong to the same cluster gradually decreases. When the location distance is greater than D_g, it is considered that there is no possibility that the two targets belong to the same cluster. Based on the definition of distance $d(\cdot)$, we give the process of the DBSCAN algorithm as follows:

B. BAYESIAN FILTERING PROCESS

In Section 2, we have obtained the motion model of the cluster target. Since a single target is affected by other targets in the same cluster and the cluster state is constantly changing, it is necessary to estimate the state of a single target on the basis of joint state estimation of all targets in the cluster. Therefore, in the process of filtering, it is necessary to divide the clusters every moment.

TABLE 2. The DBSCAN clustering algorithm [15].

Algorithm 1 DBSCAN algorithm implementation steps

Input: Uncertain data set D, Clustering radius *Eps*, Minimal number of neighboring points *MinPts*
Output: A set of clusters, types of all the points in D
Main function of the algorithm:

```
DBSCAN(D, Eps, MinPts)
  ClusterNum=0
  for each target point P in D
    if P is visited
      continue to next point
    end if
    mark P as visited
    Eps-Neighborhood=regionQuery(P, Eps)
    if sizeof(Eps-Neighborhood)<MinPts
      mark P as noise
    else
    ClusterNum=next cluster
    expandCluster(P, Eps-Neighborhood, ClusterNum, Eps, MinPts)
    end if
  end for
END
  regionQuery(P, Eps)
      return Eps-Neighborhood(P)= {Q ∈ S | D(P,Q) ≤ Eps}
    expandCluster(P, Eps-Neighborhood, ClusterNum, Eps, MinPts)
    add P to cluster ClusterNum
     for each point P' in Eps-Neighborhood
       if P' is not visited
            mark P' as visited
            Eps-Neighborhood' =regionQuery( P' , Eps)
            if sizeof( Eps-Neighborhood' )>=MinPts
Eps-Neighborhood=Eps-Neighborhood joined with Eps-Neighborhood'
            end if
       end if
       if P' is not yet member of any cluster
         add P' to cluster ClusterNum
       end if
     end for
```

At time k, there are N_m targets in the field of view and the joint state is $\boldsymbol{X}_k = \left[\boldsymbol{x}_{k,1}, \boldsymbol{x}_{k,2}, \cdots, \boldsymbol{x}_{k,N_m}\right]^T$ with measurements $\boldsymbol{Z}_k$. The cluster state estimation is $\boldsymbol{G}_k$. The measurements set from 1 to k are $\boldsymbol{Z}_{1:k} = [\boldsymbol{Z}_1, \boldsymbol{Z}_2, \cdots, \boldsymbol{Z}_k]^T$.

Assuming a Markovian state transition, the standard Bayesian filtering prediction step is given by

$$p(\boldsymbol{X}_{k+1}, \boldsymbol{G}_{k+1} | \boldsymbol{Z}_{1:k}) = \int p(\boldsymbol{X}_{k+1}, \boldsymbol{G}_{k+1} | \boldsymbol{X}_k, \boldsymbol{G}_k) p(\boldsymbol{X}_k, \boldsymbol{G}_k | \boldsymbol{Z}_{1:k}) d\boldsymbol{X}_k d\boldsymbol{G}_k \tag{37}$$

Because the prediction of joint state $\boldsymbol{X}_{k+1}$ is influenced by $\boldsymbol{G}_k$, we can obtain Equation (38) as follows:

$$p(\boldsymbol{X}_{k+1}, \boldsymbol{G}_{k+1} | \boldsymbol{X}_k, \boldsymbol{G}_k) \propto p(\boldsymbol{X}_{k+1} | \boldsymbol{X}_k, \boldsymbol{G}_k) p(\boldsymbol{G}_{k+1} | \boldsymbol{X}_{k+1}, \boldsymbol{G}_k) \tag{38}$$

$p(\boldsymbol{X}_{k+1} | \boldsymbol{X}_k, \boldsymbol{G}_k)$ is the probability density function of the joint target state transition. The motions of different clusters

are assumed mutually independent. Hence,

$$p(\boldsymbol{X}_{k+1}|\boldsymbol{X}_k, \boldsymbol{G}_k) = \prod_{j=1}^{N(\boldsymbol{G}_k)} p(\boldsymbol{X}_{k+1,j}|\boldsymbol{X}_{k,j}) \tag{39}$$

where $N(\boldsymbol{G}_k)$ is the number of clusters in the field of view at time k. If the number of targets in cluster j is $N_{g,j}$, then we can write

$$p(\boldsymbol{X}_{k+1,j}|\boldsymbol{X}_{k,j}) = \prod_{i=1}^{N_{g,j}} p(\boldsymbol{x}_{k+1,i}|\boldsymbol{x}_{k,i}) \tag{40}$$

For the resolvable target $\boldsymbol{x}_{k,i}$, the prediction density is as follows:

$$p(\boldsymbol{x}_{k+1,i}|\boldsymbol{x}_{k,i}) = \int N(\boldsymbol{x}_{k+1,i}, \boldsymbol{F}_k\boldsymbol{x}_{k,i} + \boldsymbol{\mu}^0_{k,i}, \boldsymbol{Q}^0_{k,i}) p(\boldsymbol{x}_{k,i}) d\boldsymbol{x}_{k,i} \tag{41}$$

$p(\boldsymbol{G}_{k+1}|\boldsymbol{X}_{k+1}, \boldsymbol{G}_k)$ is the discrete probability from one clustering situation to another. It reflects the ratio of a certain clustering result in all possible clustering results at time $k+1$. The clustering result of the DBSCAN clustering algorithm depends on the choice of parameters $\{D_g, \sigma_{R_v}, Eps, MinPts\}$. In order to produce all reasonable clustering results to calculate $p(\boldsymbol{G}_{k+1}|\boldsymbol{X}_{k+1}, \boldsymbol{G}_k)$, we take parameters $\{D_g, \sigma_{R_v}, Eps, MinPts\}$ as fixed parameters, and take σ_{R_v} as a changeable parameter. By changing the parameter σ_{R_v}, different clustering results are obtained by the DBSCAN clustering algorithm, and then $p(\boldsymbol{G}_{k+1}|\boldsymbol{X}_{k+1}, \boldsymbol{G}_k)$ is calculated.

The standard Bayesian filtering update step is given by

$$p(\boldsymbol{X}_{k+1}, \boldsymbol{G}_{k+1}|\boldsymbol{Z}_{1:k+1}) = \frac{p(\boldsymbol{Z}_{k+1}|\boldsymbol{X}_{k+1}, \boldsymbol{G}_{k+1}) p(\boldsymbol{X}_{k+1}, \boldsymbol{G}_{k+1}|\boldsymbol{Z}_{1:k})}{\int p(\boldsymbol{Z}_{k+1}|\boldsymbol{X}_{k+1}, \boldsymbol{G}_{k+1}) p(\boldsymbol{X}_{k+1}, \boldsymbol{G}_{k+1}|\boldsymbol{Z}_{1:k}) d\boldsymbol{X}_{k+1} d\boldsymbol{G}_{k+1}} \tag{42}$$

According to the standard association rules that a measurement originates from a target or clutter, and one target can only produce one or zero measurement, we can arrive at the likelihood probability given by

$$p(\boldsymbol{Z}_{k+1}|\boldsymbol{X}_{k+1}, \boldsymbol{G}_{k+1}) = \prod_{i=1}^{N_a} p\left(\boldsymbol{z}_{k+1,i} \mid \boldsymbol{x}_{k+1,i}\right), \quad N_a = \sum_{i=1}^{N(\boldsymbol{G}_{k+1})} N_{g,i} \tag{43}$$

$p\left(\boldsymbol{z}_{k+1,i} \mid \boldsymbol{x}_{k+1,i}\right)$ is derived by

$$p\left(\boldsymbol{z}_{k+1,i} \mid \boldsymbol{x}_{k+1,i}\right) = \mathcal{N}\left(\boldsymbol{z}_{k+1,i}, \boldsymbol{H}_{k+1}\boldsymbol{\mu}_{k+1|k,i}, \boldsymbol{R}_{k+1} + \boldsymbol{H}_{k+1}\boldsymbol{P}_{k+1,i}\right) \boldsymbol{H}^T_{k+1,i} \tag{44}$$

$$\boldsymbol{\mu}_{k+1,i} = \boldsymbol{\mu}_{k+1|k,i} + \boldsymbol{K}_{k+1,i}\left(\boldsymbol{z}_{k+1,i} - \boldsymbol{H}_{k+1}\boldsymbol{\mu}_{k+1|k,i}\right) \tag{45}$$

$$\boldsymbol{P}_{k+1,i} = \left(\boldsymbol{I} - \boldsymbol{K}_{k+1,i}\boldsymbol{H}_{k+1}\right)\boldsymbol{P}_{k+1|k,i} \tag{46}$$

$$\boldsymbol{K}_{k+1,i} = \boldsymbol{P}_{k+1,i}\boldsymbol{H}_{k+1}\left(\boldsymbol{H}_{k+1}\boldsymbol{P}_{k+1,i}\boldsymbol{H}^T_{k+1} + \boldsymbol{R}_{k+1}\right)^{-1} \tag{47}$$

C. δ-GLMB FILTER

The generalized label multi-Bernoulli (GLMB) RFS is the label RFS in state space $\mathbb{X}$ and the discrete label space $\mathbb{L}$. The GLMB process defined in C can propagate multiple hypotheses in the label sets of different trajectories, which effectively solves the problem of uncertain data association of the Bayes multi-target filter. The δ-GLMB RFS is a special form of GLMB RFS, which has a special structure in the index space. The derivation of the δ-GLMB filter is as follows:

$$\mathrm{C} = \mathcal{F}(\mathbb{L}) \times \Xi \tag{48}$$

$$\omega^{(c)}(L) = \omega^{(I,\xi)}(L) = \omega^{(I,\xi)}\delta_I(L) \tag{49}$$

$$p^{(c)} = p^{(I,\xi)} = p^{\xi} \tag{50}$$

Here, Ξ is a discrete space and ξ belongs to Ξ. I is the label set of trajectories. At time k, δ-GLMB RFS density is given by

$$\pi(X) = \Delta(X) \sum_{(I,\xi)\in F(L)\times\Xi} \omega^{(I,\xi)}\delta_I(L(X)) \left[p^{(\xi)}\right]^X \tag{51}$$

Its cardinality distribution is

$$\rho(n) = \sum_{(I,\xi)\in F(L)\times\Xi} \sum_{L\in F(L)} \omega^{(I,\xi)}\delta_I(L(X)) = \sum_{(I,\xi)\in F(L)\times\Xi} \omega^{(I,\xi)} \tag{52}$$

At time $k+1$, the δ-GLMB prediction density is given by

$$\pi_+(X_+) = \Delta(X_+) \sum_{(I_+,\xi)\in F(L_+)\times\Xi} \omega^{(I_+,\xi)}_+ \delta_{I_+}(L(X_+)) \left[p^{(\xi)}_+\right]^{X_+} \tag{53}$$

where

$$\omega^{(I_+,\xi)}_+ = \omega_B(I_+ \cap B)\,\omega^{\xi}_S(I_+ \cap L) \tag{54}$$

$$\omega^{(\xi)}_s(L) = \left[\eta^{(\xi)}_S\right]^L \sum_{I\supseteq L} \left[1 - \eta^{(\xi)}_S\right]^{I-L} \omega^{(I,\xi)} \tag{55}$$

$$\eta^{(\xi)}_S(l) = \left\langle p_S(\cdot, l), p^{(\xi)}(\cdot, l)\right\rangle \tag{56}$$

$$p^{(\xi)}_+(x, l) = 1_L(l)p^{(\xi)}_S(x, l) + 1_B(l)p_B(x, l) \tag{57}$$

$$p^{(\xi)}_S(x, l) = \frac{\left\langle p_S(\cdot, l)f(x \mid \cdot, l), p^{(\xi)}(\cdot, l)\right\rangle}{\eta^{(\xi)}_S(l)} \tag{58}$$

Note that $\omega_B(I_+ \cap B)$ is the weight of the birth labels $(I_+ \cap B)$, and $\omega^{\xi}_S(I_+ \cap L)$ is the weight of the survival labels $(I_+ \cap L)$. $f(x \mid \cdot, l)$ is a target transition density of trajectory l, and $\eta^{(\xi)}_S(l)$ is the survival probability of trajectory l. $p_B(x, l)$ is the density of the newly born target, and $p^{(\xi)}_s(x, l)$ is the predicted density of a surviving target.

The parameter set $\pi_+ = \left\{r^{(l)}_+, p^{(l)}_+\right\}_{l\in L_+}$ is obtained from the prediction step, then the δ-GLMB RFS matching the multi-target posterior density is $\pi(\cdot \mid Z) = \left\{\left(r^{(l)}, p^{(l)}\right)\right\}_{l\in \mathrm{L}_+}$.

Where

$$r^{(l)} = \sum_{(I_+,\theta)\in(F(\mathrm{L}_+)\times\Theta_{I_+})} \omega^{(I_+,\theta)}(Z)1_{I_+}(l) \tag{59}$$

$$p^{(l)}(x) = \frac{1}{r^{(l)}} \sum_{(I_+,\theta)\in F(\mathrm{L}_+)\times\Theta_I} \omega^{(I_+,\theta)}(Z)1_{I_+}(l)p^{(\theta)}(x,l) \tag{60}$$

$$\omega^{(I_+,\theta)}(Z) \propto \omega_+(I_+)\left[\eta_Z^{(\theta)}\right]^{I_+} \tag{61}$$

$$p^{(l)}(x,l \mid Z) = \frac{p_+(x,l)\psi_Z(x,l;\theta)}{\eta_Z^{(\theta)}(l)} \tag{62}$$

$$\omega^{(I_+,\theta)}(Z) \propto \omega_+(I_+)\left[\eta_Z^{(\theta)}\right]^{I_+} \tag{63}$$

$$p^{(l)}(x,l \mid Z) = \frac{p_+(x,l)\psi_Z(x,l;\theta)}{\eta_Z^{(\theta)}(l)} \tag{64}$$

$$\eta_Z^{(\theta)}(l) = \langle p_+(\cdot,l), \psi_z(\cdot,l;\theta)\rangle \tag{65}$$

$$\psi_z(x,l;\theta) = \begin{cases} \dfrac{p_D(x,l)g\left(z_{\theta(l)} \mid x,l\right)}{\kappa\left(z_{\theta(l)}\right)}, & \theta(l) > 0 \\ q_D(x,l), & \theta(l) = 0 \end{cases} \tag{66}$$

Θ_{I_+} is the space of mapping θ: $I_+ \to \{0,1,\cdots,|Z|\}$. Therefore, $\theta(i) = \theta\left(i'\right) > 0$ means $i = i'$. $p_D(x,l)$ is the detection probability of (x,l), and $q_D(x,l)$ is the missed detection probability of (x,l). $g(z \mid x,l)$ is the likelihood function, and $\kappa(\cdot)$ is the Poisson clutter density.

The multi-target tracking method based on RFS should use a specific execution method when it is implemented. Commonly used execution methods include the sequential Monte Carlo (SMC) method, the Gaussian mixture approximation (GM) method, and methods based on nonlinear Kalman filter. For the target model established in this paper, although the model is established on the CV model, it has nonlinear characteristics because of the collaborative noise. Since the unscented Kalman Filter (UKF) is more robust to nonlinearity than the extended Kalman filter (EKF), the UKF is selected as the execution algorithm in this paper. Reference [5] gives a detailed algorithm flow.

IV. EXPERIMENTS AND RESULTS

In this section, three simulation experiments are conducted to verify the effectiveness of the proposed tracking algorithm. The experimental scenarios include the merging of clusters, the splitting of clusters, and the reorganization of some targets in the cluster. In these experiments, it is assumed that the sensor can fully resolve and continuously track cluster targets. In all simulations, the cluster motion model parameters are set as shown in Table 3. The target state vector is

$$\boldsymbol{x} = \left[x\ \dot{x}\ y\ \dot{y}\right]^T.$$

The target state and measurement equation are shown in Equations (28, 29). Setting the covariance matrix of measurement noise is $\boldsymbol{R}_k = diag\,[0.25\ 0.25]^T$. The clutter obeys the Poisson distribution with parameter $\lambda_c = 15$. Set $p_D = 0.98$, $p_s = 0.99$ and $\boldsymbol{S}_k = diag\left[6.25\times10^{-8}, 2.5\times10^{-7}, 6.25\times10^{-8}, 2.5\times10^{-7}\right]^T$.

TABLE 3. Cluster motion model parameters for simulations.

$\alpha = 0.05$	$\beta = 0.1$	$d_r = 10$	$d_m = 20$	$R_{11} = 2$
$R_{12} = 2$	$R_{21} = 2$	$R_{22} = 2$	$\sigma_x = \sigma_y = 0.005$	$\sigma_g = 0.005$

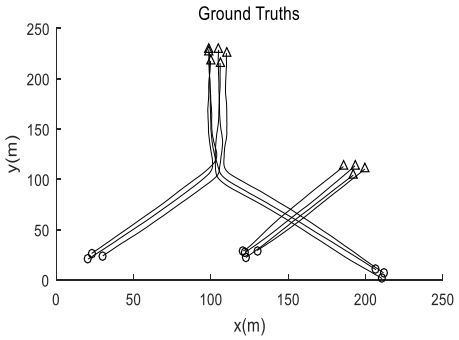

FIGURE 6. The trajectory of cluster targets.

TABLE 4. Cluster motion process information in Scenario 1.

	Cluster 1	Cluster 3	Cluster 2
Appearing time k_a	30	1	20
Disappearing time k_d	Merging time k_d =300		120
Number of targets	3	3	4
Initial position	$[20,30]\times[20,30]$	$[205,215]\times[0,10]$	$[120,130]\times[20,30]$
Initial velocity $[\dot{x},\dot{y}]^T$	$\left[\frac{1}{\sqrt{2}},\frac{1}{\sqrt{2}}\right]^T$	$\left[\frac{-1}{\sqrt{2}},\frac{1}{\sqrt{2}}\right]^T$	$\left[\frac{1}{\sqrt{2}},\frac{1}{\sqrt{2}}\right]^T$

A. EXPEROMENTAL SCENARIO 1: THE MERGING OF CLUSTERS

In this subsection, we track the merging process of clusters. There are three cluster motions in the sensor field of view $[0,250]\times[0,250]\,(m^2)$ shown in Figure 6. Along the x-axis, they are Cluster 1, Cluster 2, and Cluster 3, respectively. The appearing time, initial position, and velocity of the three clusters are shown in the Table 4. In the sensor field of view, Cluster 1 and Cluster 3 merge and Cluster 2 and Cluster 3 cross as the clusters move. The trajectory of the targets is shown in Figure 6. Where the curve shows the trajectory, the circle represents the starting point, and the triangle is the end points.

Figure 7 shows the tracking results of cluster targets in experimental Scenario 1. It can be seen that there are many measuring points at each moment, including true measurements, and much clutter. Most of the position estimation points are close to the true position points. However, there are still some position estimation points that are quite different

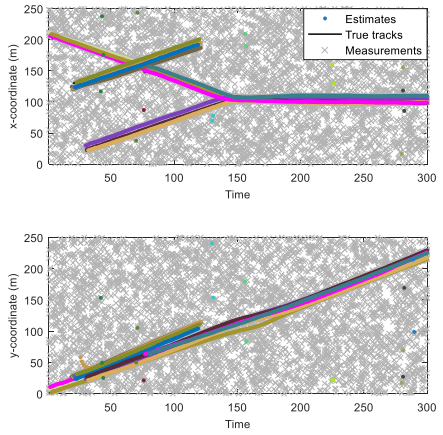

FIGURE 7. Tracking results of targets.

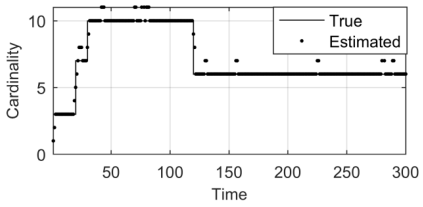

FIGURE 8. The estimated number of targets.

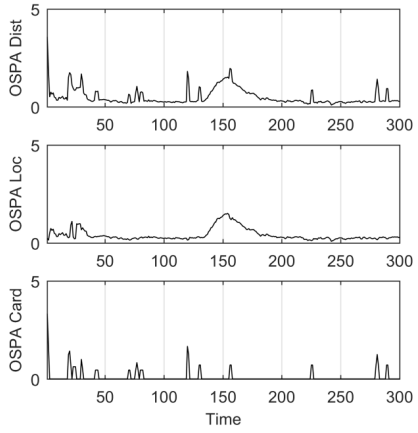

FIGURE 9. The OSPA distance.

from the true position points, which will be recognized as noise points by the DBSCAN algorithm. This will avoid the influence of these points on calculating the mean and variance of the collaborative noise in the prediction process.

Optimal sub-pattern assignment (OSPA) [33] is a common index to evaluate the tracking effect of the RFS tracking method. Setting the OSPA distance calculation parameters $c = 5$ and $p = 1$, we get the OSPA distance shown in Figure 9.

At the beginning of tracking, targets appear one after another, and OSPA distance fluctuates greatly. At about time $k = 150$, Cluster 1 and Cluster 3 merge. Although one cluster has been affected by the potential force of another cluster in the initial stage of merging, the effect is not enough to

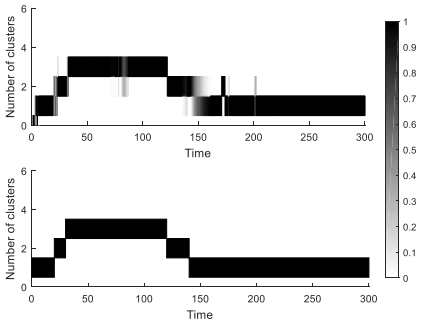

FIGURE 10. The estimated number of clusters and the probability of corresponding number.

TABLE 5. Cluster motion process information in Scenario 2.

	Cluster 1	Cluster 2
Appearing time k_a	1	30
Splitting time k_s	100	130
Disappearing time k_d	200	180
Number of targets	6	6
Initial position	$[100,110]\times[0,10]$	$[50,60]\times[0,10]$
Initial velocity $[\dot{x},\dot{y}]^T$	$[0,1]^T$	$\left[\frac{1}{\sqrt{2}},\frac{1}{\sqrt{2}}\right]^T$

make its velocity change significantly. Under the selected parameter σ_{R_v}, the DBSCAN algorithm is not sensitive to this change of velocity, which leads to the fluctuation of OSPA Loc. When the merging process of the two clusters is finished, the DBSCAN algorithm divides these targets into a cluster correctly. The cooperative interaction of each target is calculated accurately, and OSPA Loc is reduced.

Setting the DBSCAN algorithm fixed parameters $D_g = 20$, $Eps = 20$, and $MinPts = 20$. The changeable parameter σ_{R_v} increases from 0.2 to 1 in increments of 0.01. The number of clusters and the probability of the corresponding number are shown in Figure 10. In the figure, the true number of clusters is at the bottom, and the estimated by the DBSCAN algorithm is at the top. It can be seen that the DBSCAN algorithm can effectively divide the targets in the sensor field of view. It is evident that cluster merging is not completed in an instant but within a period of time. The DBSCAN algorithm with a changeable parameter can effectively describe this process within time 140-160.

B. EXPEROMENTAL SCENARIO 2: THE SPLITTING OF CLUSTERS

In this subsection, we track the splitting process of clusters. At the beginning, there are two clusters in the sensor field of view $[0, 200] \times [0, 300]$ (m^2) shown in Figure 11(a). Along the x-axis, they are Cluster 1 and Cluster 2, respectively. As the clusters move, Cluster 1 and Cluster 2 receive splitting instructions. Cluster 1 splits to produce 3 sub-clusters, and Cluster 2 splits to produce 2 sub-clusters. The splitting process is a circular motion with an angular velocity $\omega_s = \frac{\pi}{60} rad/s$ and continues $10s$. The motion process of clusters is shown in Table 5.

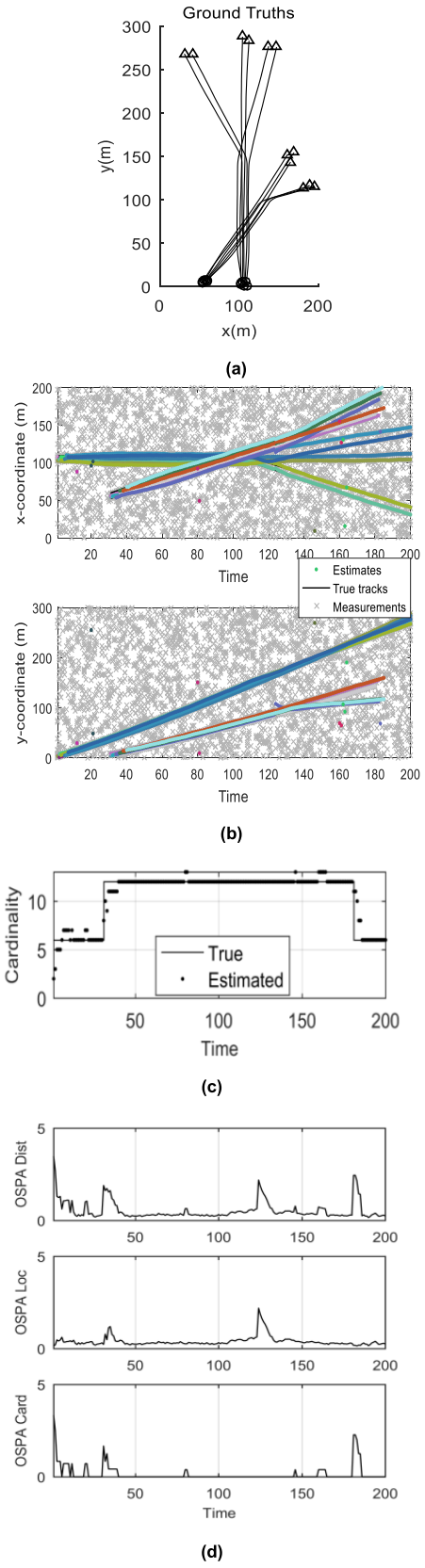

FIGURE 11. The result of tracking the splitting of clusters. (a) is the trajectory of cluster targets; (b) is the tracking results of the targets; (c) is the estimated number of targets; (d) is the OSPA distance.

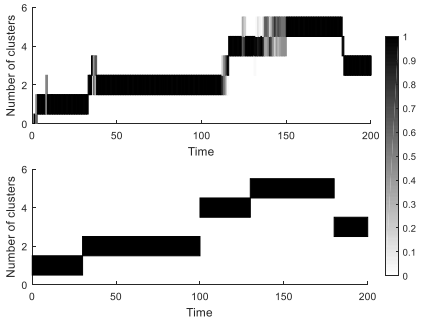

FIGURE 12. The estimated number of clusters and the probability of a corresponding number.

TABLE 6. Cluster motion process information in Scenario 3.

	Cluster 1	Cluster 2
Appearing time k_a	1	20
Disappearing time k_s	Partially disappearing 100 Totally disappearing 150	120
Numbers of targets	8	4
Initial position	$[0,10]\times[0,10]$	$[70,80]\times[10,20]$
Initial velocity $[\dot{x},\dot{y}]^T$	$\left[\frac{1}{\sqrt{2}},\frac{1}{\sqrt{2}}\right]^T$	$\cdot\left[\frac{-1}{\sqrt{2}},\frac{1}{\sqrt{2}}\right]^T$

The results of target tracking, target number estimation, and OSPA distance are shown in Figure 11(b), 11(c), and 11(d). It can be seen that the OSPA Loc increases at the time of cluster splitting. This is mainly caused by the inability of the CV model to adapt to the turning motion. After the turning process, the DBSCAN algorithm can correctly divide the targets and the OSPA Loc is reduced.

We set the DBSCAN algorithm fixed parameters $D_g = 20$, $Eps = 20$, and $MinPts = 20$. Because of the small splitting angular velocity, in order to improve the sensitivity of the DBSCAN algorithm to the change of velocity direction, the changeable parameter σ_{R_v} increases from 0.2 to 0.4 in increments of 0.01. The clustering result is shown in Figure 12. It can be seen that when a cluster splits into multiple sub-clusters or multiple clusters disappear at the same time, the response of the algorithm to the number of clusters is delayed. But soon after the split starts, the algorithm can identify the number of clusters in the field of view.

C. EXPEROMENTAL SCENARIO 3: THE REORGANIZATION OF CLUSTERS

In this subsection, we track the reorganization process of targets in a cluster. The reorganization process occurs when some targets suddenly disappear in the cluster. At the beginning, there are two clusters in the sensor field of view $[0, 150] \times [0, 150]\,(m^2)$ shown in Figure 13(a). At about time 65, Cluster 1 and Cluster 2 cross. At time 100, some targets disappear in Cluster 1, and the others reorganize with changing velocity due to the cooperative interaction. The motion process of clusters is shown in Table 6.

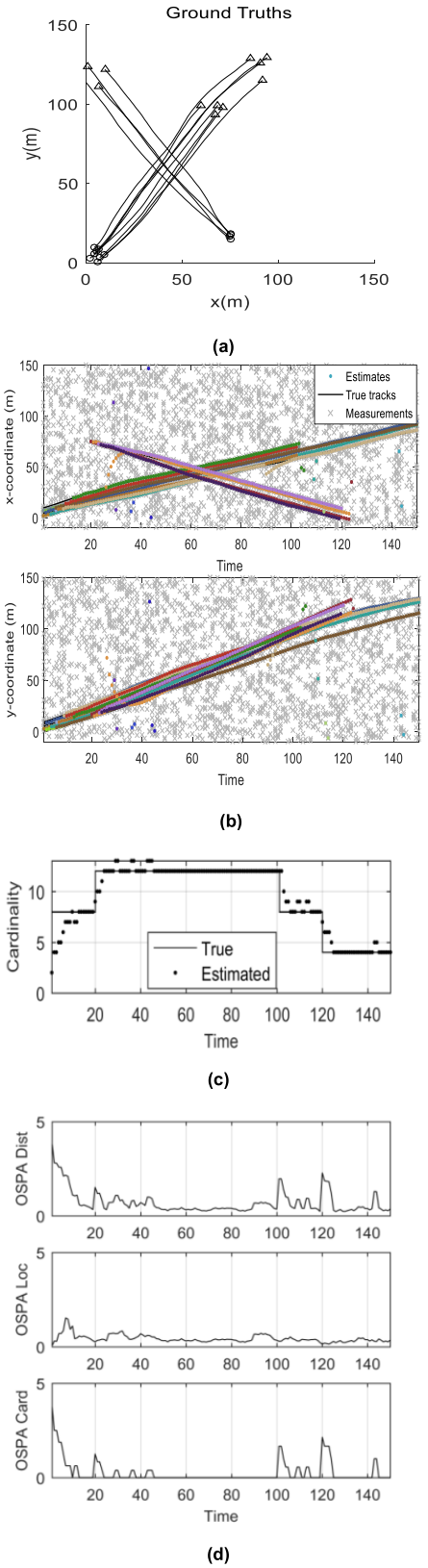

FIGURE 13. The result of tracking the reorganization of clusters. (a) is the trajectory of cluster targets; (b) is the tracking results of targets; (c) is the estimated number of targets; (d) is the OSPA distance.

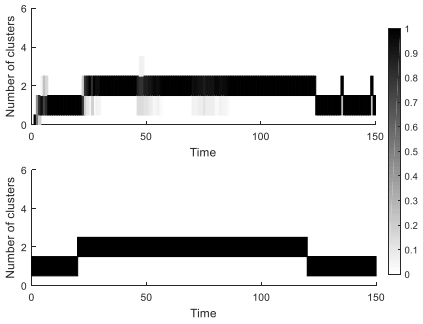

FIGURE 14. The estimated number of clusters and the probability of corresponding number.

The results of target tracking, target number estimation, and OSPA distance are shown in Figures 13(b), 13(c), and 13(d). It can be seen that the OSPA Loc is always small, and that the tracking algorithm can adapt to the reorganization of the targets.

We set the DBSCAN algorithm fixed parameters to $D_g = 20$, $Eps = 20$, and $MinPts = 20$. The changeable parameter σ_{R_v} increases from 0.2 to 0.8 in increments of 0.01. The clustering result is shown in Figure 14. It can be seen from the figure that the DBSCAN algorithm can still guarantee a high probability of correct clustering even if many targets cross each other at about time 65.

V. CONCLUSION

In this paper, we use stochastic differential equations to model the cooperative interaction of the cluster and derive the state equation of the cluster targets. We redefine the DBSCAN algorithm distance measure according to the characteristics of the cluster targets and realize the division of targets in the field of view by the DBSCAN algorithm. We combine the DBSCAN algorithm with the prediction step of the δ-GLMB filter to realize the state estimation of targets and clusters at the same time. In the experiments, we simulate the merging, splitting, and reorganization behavior of targets and track the cluster targets by the proposed method. The results show that the method proposed in this paper can effectively identify the behaviors of cluster targets, estimate the interaction of the targets, and accurately track the targets. However, because the target state equation in this paper is based on the CV model, the tracking algorithm is difficult to adapt to the more complex motion of the cluster targets. In the next step, we consider applying the interactive multiple model (IMM) algorithm to track cluster targets.

APPENDIX

Consider the following energy function:

$$E = \sum_{i=1}^{N} \sum_{\forall j, j \neq i} U_j \left(\left\| \boldsymbol{s}_{t,i} - \boldsymbol{s}_{t,j} \right\| \right) + \frac{1}{2} \sum_{i=1}^{N} \dot{\boldsymbol{s}}_{t,i}^T \dot{\boldsymbol{s}}_{t,i} \quad \text{(A.1)}$$

The level set $\Omega_c = \left\{ \left(\left\| \boldsymbol{s}_{t,i} - \boldsymbol{s}_{t,j} \right\|, \dot{\boldsymbol{s}}_{t,i} \right) \middle| E \leq c, c > 0 \right\}$ is defined as the compact set on the relative distance between

cluster members and the velocity space. From the continuity, we can see that Ω_c is a closed set. Because of $E \leq c$, we can arrive at $U_j\left(\left\|\boldsymbol{s}_{t,i}-\boldsymbol{s}_{t,j}\right\|\right) \leq c, \dot{\boldsymbol{s}}_{t,i}^T \dot{\boldsymbol{s}}_{t,i} \leq 2c$. Since $U_j\left(\left\|\boldsymbol{s}_{t,i}-\boldsymbol{s}_{t,j}\right\|\right) \leq c$ and the cluster topology has weak connectivity, $\exists R > 0$ makes $\left\|\boldsymbol{s}_{t,i}-\boldsymbol{s}_{t,j}\right\| \leq R$. Because of $\dot{\boldsymbol{s}}_{t,i}^T \dot{\boldsymbol{s}}_{t,i} \leq 2c$, there is $\left\|\boldsymbol{s}_{t,i}\right\| \leq \sqrt{2c}$. Thus Ω_c is a bounded closed positive invariant set.

Without considering the effect of noise, the control input of cluster members can be considered as follows:

$$u_{t,i} = \frac{d\dot{\boldsymbol{s}}_{t,i}}{dt} = -\alpha\left[\dot{\boldsymbol{s}}_{t,i} - f\left(\dot{\boldsymbol{s}}_t\right)\right] + r_i\left(\boldsymbol{s}_{t,i}\right) \tag{A.2}$$

By calculating the time derivative of the energy function, the following equation can be obtained.

$$\begin{aligned}\dot{E} &= \sum_{i=1}^{N}\left[-\sum_{\forall j, j\neq i}\dot{\boldsymbol{s}}_{t,i}^T r\left(\boldsymbol{s}_{t,i}, \boldsymbol{s}_{t,j}\right) + \dot{\boldsymbol{s}}_{t,i}^T u_{t,i}\right] \\ &= -\alpha\sum_{i=1}^{N}\dot{\boldsymbol{s}}_{t,i}^T\left[\dot{\boldsymbol{s}}_{t,i} - f\left(\dot{\boldsymbol{s}}_t\right)\right]\end{aligned} \tag{A.3}$$

Because of $\sum_{i=1}^{N}\dot{\boldsymbol{s}}_{t,i}^T\left[\dot{\boldsymbol{s}}_{t,i} - f\left(\dot{\boldsymbol{s}}_t\right)\right] = \frac{1}{N}\sum_{i=1}^{N}\sum_{j=i+1}^{N}\left(\dot{\boldsymbol{s}}_{t,i} - \dot{\boldsymbol{s}}_{t,j}\right)^2 \geq 0$, we can get $\dot{E} \leq 0$.

According to the LaSalle invariant set principle, any solution of the system starting from the level set will converge to the largest invariant set in set $Q = \left\{\left(\left\|\boldsymbol{s}_{t,i}-\boldsymbol{s}_{t,j}\right\|, \dot{\boldsymbol{s}}_{t,i}\right) \in \Omega_c \middle| \dot{E} = 0\right\}$. The velocity of cluster members can gradually become consistent to form a collective motion.

ACKNOWLEDGMENT

The authors contributed significantly to the writing and final editing of the manuscript. Xirui Xue conceived the ideas of theory and finally edited the article. Shucai Huang, Jiahao Xie, Jiashun Ma, and Ning Li checked and corrected the article.

REFERENCES

[1] J. W. Koch, "Bayesian approach to extended object and cluster tracking using random matrices," *IEEE Trans. Aerosp. Electron. Syst.*, vol. 44, no. 3, pp. 1042–1059, Jul. 2008.
[2] S. K. Pang, J. Li, and S. J. Godsill, "Detection and tracking of coordinated groups," *IEEE Trans. Aerosp. Electron. Syst.*, vol. 47, no. 1, pp. 472–502, Jan. 2011.
[3] X. Ru, Y. Chi, and W. Liu, "A detection and tracking algorithm for resolvable group with structural and formation changes using the gibbs-GLMB filter," *Sensors*, vol. 20, no. 12, p. 3384, Jun. 2020.
[4] W. Liu, S. Zhu, C. Wen, and Y. Yu, "Structure modeling and estimation of multiple resolvable group targets via graph theory and multi-Bernoulli filter," *Automatica*, vol. 89, pp. 274–289, Mar. 2018.
[5] Y. Chi and W. Liu, "Resolvable group state estimation with maneuver movement based on labeled RFS," in *Proc. Int. Conf. Control, Autom. Inf. Sci. (ICCAIS)*, Hangzhou, China, Oct. 2018, pp. 249–254.
[6] C. W. Reynolds, "Flocks, herds and schools: A distributed behavioral model," in *Proc. 14th Annu. Conf. Comput. Graph. Interact. Techn.*, Anaheim, CA, USA, 1987, pp. 25–34.
[7] T. Vicsek, A. Czirók, E. Ben-Jacob, I. Cohen, and O. Shochet, "Novel type of phase transition in a system of self-driven particles," *Phys. Rev. Lett.*, vol. 75, no. 6, pp. 1226–1229, Aug. 1995.
[8] I. D. Couzin, J. Krause, N. R. Franks, and S. A. Levin, "Effective leadership and decision-making in animal groups on the move," *Nature*, vol. 433, no. 7025, pp. 513–516, Feb. 2005.
[9] P. Romanczuk, M. Bär, W. Ebeling, B. Lindner, and L. Schimansky-Geier, "Active Brownian particles," *Eur. Phys. J. Special Topics*, vol. 202, no. 1, pp. 1–162, Mar. 2012.
[10] A. Mogilner, L. Bent, A. Spiros, and L. Edelstein-Keshet, "Mutual interactions, potentials, and individual distance in a social aggregation," *J. Math. Biol.*, vol. 47, no. 4, pp. 353–389, Sep. 2003.
[11] N. Shimoyama, K. Sugawara, and T. Mizuguchi, "Collective motion in a system of motile elements," *Phys. Rev. Lett.*, vol. 76, no. 20, p. 3870, May 1996.
[12] S. G. Meester and J. MacKay, "A parametric model for cluster correlated categorical data," *Biometrics*, vol. 50, pp. 954–963, Dec. 1994.
[13] S. C. Johnson, "Hierarchical clustering schemes," *Psychometrika*, vol. 32, no. 3, pp. 241–254, Sep. 1967.
[14] J. MacQueen, "Some methods for classification and analysis of multivariate observations," in *Proc. 5th Berkeley Symp. Math. Statist. Probab.*, Berkeley, CA, USA, 1967, pp. 281–297.
[15] M. Ester, H. P. Kriegel, J. Sander, and X. W. Xu, "A density-based algorithm for discovering clusters a density-based algorithm for discovering clusters in large spatial databases with noise," in *Proc. 2nd Int. Conf. Knowl. Discovery Data Mining*, Portland, OR, USA, Aug. 1996, pp. 2–4.
[16] X. Zhang, H. Liu, and X. Zhang, "Novel density-based and hierarchical density-based clustering algorithms for uncertain data," *Neural Netw.*, vol. 93, pp. 240–255, Sep. 2017.
[17] L. Mihaylova, A. Y. Carmi, F. Septier, A. Gning, S. K. Pang, and S. Godsill, "Overview of Bayesian sequential Monte Carlo methods for group and extended object tracking," *Digit. Signal Process.*, vol. 25, pp. 1–16, Feb. 2014.
[18] F. Septier, S. K. Pang, S. Godsill, and A. Carmi, "Tracking of coordinated groups using marginalised MCMC-based particle algorithm," in *Proc. IEEE Aerosp. Conf.*, Montana, Helena, Mar. 2009, pp. 1–11.
[19] S. K. Pang, J. Li, and S. J. Godsill, "Models and algorithms for detection and tracking of coordinated groups," in *Proc. IEEE Aerosp. Conf.*, Montana, Helena, Mar. 2008, pp. 1–17.
[20] A. Gning, L. Mihaylova, S. Maskell, S. K. Pang, and S. Godsill, "Group object structure and state estimation with evolving networks and Monte Carlo methods," *IEEE Trans. Signal Process.*, vol. 59, no. 4, pp. 1383–1396, Apr. 2011.
[21] S. S. Blackman, "Multiple hypothesis tracking for multiple target tracking," *IEEE Aerosp. Electron. Syst. Mag.*, vol. 19, no. 1, pp. 5–18, Jan. 2004.
[22] L. Svensson, D. Svensson, M. Guerriero, and P. Willett, "Set JPDA filter for multitarget tracking," *IEEE Trans. Signal Process.*, vol. 59, no. 10, pp. 4677–4691, Oct. 2011.
[23] K. Granstrom and U. Orguner, "A phd filter for tracking multiple extended targets using random matrices," *IEEE Trans. Signal Process.*, vol. 60, no. 11, pp. 5657–5671, Nov. 2012.
[24] K. Granstrom, P. Willett, and Y. Bar-Shalom, "PHD filter with approximate multiobject density measurement update," in *Proc. 18th Int. Conf. Inf. Fusion*, Washington, DC, USA, Jul. 2015, pp. 6–9.
[25] R. P. S. Mahler, B.-T. Vo, and B.-N. Vo, "CPHD filtering with unknown clutter rate and detection profile," *IEEE Trans. Signal Process.*, vol. 59, no. 8, pp. 3497–3513, Aug. 2011.
[26] G. Battistelli, L. Chisci, C. Fantacci, A. Farina, and A. Graziano, "Consensus CPHD filter for distributed multitarget tracking," *IEEE J. Sel. Topics Signal Process.*, vol. 7, no. 3, pp. 508–520, Jun. 2013.
[27] B.-T. Vo, B.-N. Vo, and A. Cantoni, "The cardinality balanced multi-target multi-Bernoulli filter and its implementations," *IEEE Trans. Signal Process.*, vol. 57, no. 2, pp. 409–423, Feb. 2009.
[28] J. Yin, J. Zhang, and J. Zhao, "The Gaussian particle multi-target multi-Bernoulli filter," in *Proc. 2nd Int. Conf. Adv. Comput. Control*, Shenyang, China, 2010, pp. 556–560.
[29] B.-T. Vo and B.-N. Vo, "Labeled random finite sets and multi-object conjugate priors," *IEEE Trans. Signal Process.*, vol. 61, no. 13, pp. 3460–3475, Jul. 2013.
[30] B.-N. Vo, B.-T. Vo, and D. Phung, "Labeled random finite sets and the bayes multi-target tracking filter," *IEEE Trans. Signal Process.*, vol. 62, no. 24, pp. 6554–6567, Dec. 2014.
[31] H. Yu, Y. Wang, and L. Cheng, "Flocking motion control of flock in directed networks," *Control Theory Appl.*, vol. 24, pp. 79–83, Dec. 2007.
[32] B. Oksendal, *Stochastic Differential Equations: An Introduction With Applications*. Springer, 2013.
[33] D. Schuhmacher, B.-T. Vo, and B.-N. Vo, "A consistent metric for performance evaluation of multi-object filters," *IEEE Trans. Signal Process.*, vol. 56, no. 8, pp. 3447–3457, Aug. 2008.

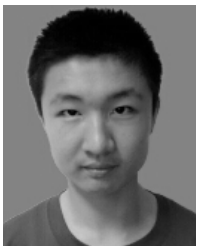

XIRUI XUE was born in 1997. He received the bachelor's degree in automation from Air Force Engineering University, Xi'an, Shaanxi, China, in 2019, where he is currently pursuing the Ph.D. degree in control science and engineering. His current research interests include target detection, target tracking, swarm intelligence, and its applications.

SHUCAI HUANG was born in Huangmei, Hubei, China, in 1967. He received the Ph.D. degree from the Air and Missile Defense College, Air Force Engineering University, Xi'an, Shaanxi, China, in 2005. He is currently a Professor with the Air and Missile Defense College. He is also a Professor and a Doctoral Supervisor. His main research interests include aerospace target cooperative tracking and interception cueing technology.

JIAHAO XIE was born in 1996. He received the bachelor's degree from the School of Mechanical Engineering, Hebei University of Technology, Tianjin, China, in 2017, and the master's degree from the Air and Missile Defense College, Air Force Engineering University, Xi'an, Shaanxi, China, in 2020, where he is currently pursuing the Ph.D. degree with the Air and Missile Defense College. His research interests include multi-objective tracking and information fusion.

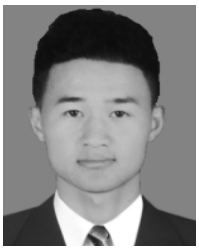

JIASHUN MA was born in 1996. He received the B.S. degree from Xi'an Polytechnic University, in 2019. He is currently pursuing the M.Sc. degree with Air Force Engineering University, Xi'an, China. His current research interests include target early warning and situation assessment.

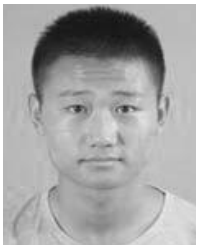

NING LI was born in 1996. He received the B.S. degree from the Hefei University of Technology, in 2019. He is currently pursuing the M.S. degree with Air Force Engineering University, Xi'an, Shaanxi, China. His current research interest includes the application of deep learning in target detection.